Scripta Materialia 166 (2019) 73–77

Contents lists available at ScienceDirect

Scripta Materialia

journal homepage: www.elsevier.com/locate/scriptamat

Strength and ductility of bulk Cu/Nb nanolaminates exposed to extremely high temperatures

Wenfan Yang [a,b], Irene J. Beyerlein [c], Qianqian Jin [a,b], Hualong Ge [a,b], Ting Xiong [a,b], Lixin Yang [a,b], Jianchao Pang [a,b], Yangtao Zhou [a,b], Xiaohong Shao [a,b], Bo Zhang [a,b], Shijian Zheng [a,d,e,*], Xiuliang Ma [a,b,f]

[a] Shenyang National Laboratory for Materials Science, Institute of Metal Research, Chinese Academy of Sciences, 72 Wenhua Road, Shenyang 110016, China
[b] School of Material Science and Engineering, University of Science and Technology of China, Hefei 230026, China
[c] Mechanical Engineering Department, Materials Department, University of California at Santa Barbara, Santa Barbara, CA 93106, USA
[d] School of Materials Science and Engineering, Research Institute for Energy Equipment Materials, Hebei University of Technology, Tianjin 300130, China
[e] Tianjin Key Laboratory of Materials Laminating Fabrication and Interface Control Technology, Hebei University of Technology, Tianjin 300130, China
[f] School of Material Science and Engineering, Lanzhou University of Technology, 730050 Lanzhou, China

ARTICLE INFO

Article history:
Received 26 January 2019
Received in revised form 5 March 2019
Accepted 5 March 2019
Available online xxxx

Keywords:
Cu-Nb
Interface
Strength
Thermal stability
Hall-Petch relation

ABSTRACT

In this work, we investigate the tensile strength and ductility of bulk Cu/Nb nanolaminates after exposure to high temperatures. We show that the interface transforms from flat to wavy at a transition temperature of 700 °C, and tensile strength is linearly proportional to $H^{-1/2}$ (H = layer thickness). Moreover, the wavy interfaces give rise to a higher slope of the Hall-Petch law. This result can be attributed to greater resistance to slip transmission across wavy interfaces compared to planar interfaces. After 1000 °C for 1 h, the material still exhibits a high strength of 468 MPa and enhanced elongation.

Cu/Nb bimetal nanolaminates are well known for both exceptional strength and thermal stability compared to their single-phase counterparts [1,2]. The superior strength has long been attributed notionally to the high density of interfaces, which act as barriers to the glide of dislocations. The outstanding thermal stability has been attributed to the high thermal stability of the biphase interface relative to grain boundaries.

Thermal stability of nanolaminates depends on microstructural stability against elevated temperatures. There naturally exists a limit temperature at which the initial microstructure is not retained. Many works have explored microstructural changes beyond the limit, such as nanolaminated Cu/Nb sheets rolled by accumulative roll bonding (ARB) [3–7] and nanolayered Cu/Nb wires fabricated by bundle drawing [8–12], giving similar results that the microstructures remain stable until 500 °C. ARB Cu/Nb nanolaminates have extremely elongated grains with grain aspect ratio exceeds 30 [4] in the rolling direction due to the deformation processing. Owing to Rayleigh instability, thinning at periodic intervals along the layer starting from annealing at 500 °C for 1 h, giving the ARB Cu/Nb interfaces a sinusoidal morphology [5].

The common viewpoint for pure metals is that when the grain size increases as a result of long time exposure to high temperatures, the material properties will degrade. For nanolaminates, in particular, the strength depends sensitively on layer thickness [13,14]. But, many factors undoubtedly can affect dislocation motion and contribute to the strength and layer size scaling on strength of the nanolaminate apart from layer thickness [15,16]. Understanding the effects of interface properties apart from layer thickness effects has been challenged by two aspects.

First, the origin of the size scaling in layer thickness H on strength is currently being researched. When layers are extremely fine, $H < 10$ nm, close to the core of a dislocation, a dislocation cannot glide within the layer but must attempt to transmit from layer to layer across the interface, and in this event the critical stress for slip transfer τ^* has little dependence on layer thickness. In an intermediate regime, $10\ \text{nm} < H < 50$ nm, the dislocations will tend to thread through the layers, a motion called confined layer slip (CLS). Molecular dynamics simulations and in-situ transmission electron microscopy (TEM) observations have indicated that when the layers are within 10 nm to 50 nm, the dislocations will tend to thread through the layers [17,18]. In this case, the stress for propagation depends on layer thickness, roughly $\sigma \sim k\log(H)/H + f$, where f depends on dislocation/interface interactions [14]. For larger

* Corresponding author at: Shenyang National Laboratory for Materials Science, Institute of Metal Research, Chinese Academy of Sciences, 72 Wenhua Road, Shenyang 110016, China.
E-mail address: sjzheng@imr.ac.cn (S. Zheng).

https://doi.org/10.1016/j.scriptamat.2019.03.007
1359-6462/

values of H, dislocations may pile up in the layer, and the stress for dislocations to propagate from layer to layer across the interface scales as $\sigma \sim K/H^{1/2}$. The coefficient K determines the sensitivity of strength to H and it has been proposed to scale with τ^*.

Second, understanding the key variables responsible for size scalings in strength has been complicated by the numerous ways in which measures of strength have been obtained. In a majority of studies, evaluating the strength of nanolaminates involved nanoindentation or micropillar compression, since these tests allow for quantifying the strength of the material when only small volumes can be made, such as by physical vapor deposition. Nanoindentation hardness testing shows that the hardness increases as H decreases, following $H^{-1/2}$ [13,14], over a wide range of H from 600 nm to a few nm, below which further decreases in H lead to weaker material. The advantage of nanolaminates made by metal forming processes, such as ARB, is that there is sufficient material to carry out meaningful strength evaluations and obtain the full deformation response. Room temperature tensile testing of Cu/Nb was carried out recently by Nizolek et al. on samples made by ARB [19]. The tensile tests showed continue strengthening with reductions in H from 1800 nm to 15 nm, also scaling as $H^{-1/2}$.

Although there is no universally accepted theory for the size scaling on strength, many of the models, simulations, and in-situ observations point to interface properties as affecting the scaling law in strength. In this work, we aim to understand the effect of interface morphology on the strength and ductility of nanolaminates and in particular the size scaling in strength. To this end, we evaluate the tensile properties of an ARB Cu/Nb nanolaminate after exposure to unusually high temperatures. Here we show that for a wide range of layer thicknesses from 32 nm to 357 nm, the tensile strength follows a Hall-Petch scaling law, despite significant changes in stored dislocation density, interface roughness, and grain size. Most importantly, we show that the scaling coefficient K depends on interface morphology, planar vs. wavy.

The Cu/Nb nanolaminate studied here is a 300 μm-thick rolled sheet with a nominal layer thickness of 32 nm. Details on the fabrication ARB process can be found in [1]. For mechanical and thermal tests, the as-rolled sheet was cut into small pieces. These small pieces were exposed to extreme temperatures in a vacuum furnace that ranged from 500 to 1000 °C for 1 h.

To analyze the microstructural changes resulting from the heat exposure, we used TEM with an FEI Tecnai F30. The TEM samples were observed in the rolling direction (RD). For post mechanical properties, we measured uniaxial tensile response. Sheets were cut into dog-bone shaped tensile samples with a gauge size of 5 mm (length)×1.5 mm (width)×0.25 mm (thickness). Uniaxial tensile tests were performed on an Instron 5848 Micro-Tester system with a strain rate of $5\times10^{-4}\,s^{-1}$ at ambient temperature. The tensile axis was parallel to the transverse direction (TD).

Fig. 1 compares the tensile stress-strain curves of the annealed samples for different annealing temperatures and Table 1 the corresponding ultimate tensile strengths and percent elongation. Two distinct groups can be noticed. For samples exposed to 500–700 °C, the ductility (e.g., elongation to failure) became progressively lower than that of the as-rolled material, which is 2.8%, as the annealing temperature increased. For 700 °C, the tensile strength and ductility decreased to 880 MPa and 1.5%, respectively. For samples exposed to 800–1000 °C, the elongation to failure was larger than that of the as-rolled material. Another distinction is the substantial drop in strength with increase in annealing temperature from 700 °C to 800 °C. Specifically at 800 °C, the tensile strength dropped 22% to 687 MPa. This reduction is larger than any other with a 100 °C change in annealing temperature. The trend is similar to Cu/Nb wires annealed at different temperatures, which shows sharp reduction in hardness around 800 °C due to recrystallization of both phases [9,11].

It is worth noting that the sample exposed to the extreme temperature, 1000 °C, has a flow stress of ~468 MPa and elongation of 6.4%.

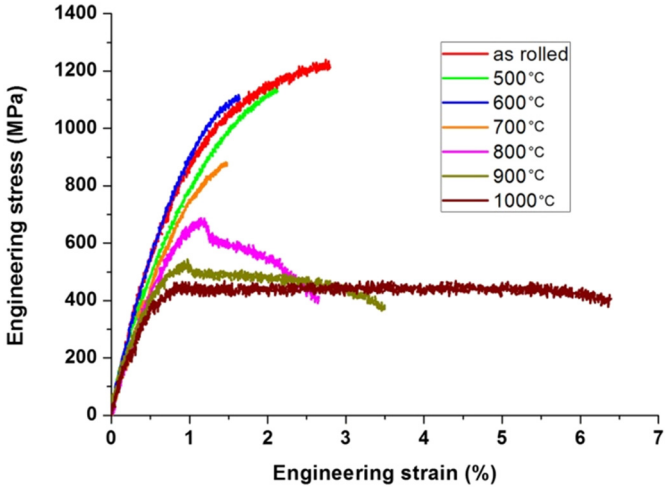

Fig. 1. Stress-strain curves of samples annealed at different temperatures for 1 h.

While it is much lower than the strength of the as-rolled material, this strength is still more than twice that of the Cu alone. A similar result has also been achieved in roll-bonded Cu/Nb, in which an ultimate tensile strength of ~466 MPa was achieved after annealing at 926 °C [20]. Therefore, high density of heterogeneous interfaces, which retard recovery and recrystallization effectively, make these Cu/Nb nanolaminates possess outstanding thermal stability compared with single phase nanocrystalline materials [9].

From the above, two results would not be anticipated: the minimum in ductility achieved at 700 °C, and the significant drop in yield strength from 700 °C to 800 °C. To understand these two results, TEM analysis was carried out on the annealed samples at each temperature. Fig. 2 shows images, showing typical changes in the interlayer grain shape, interface morphology, and layer size. For comparison, the as-rolled material had an average layer thickness of 32 nm, planar interfaces, one grain spanning the layer thickness, and elongated grains exceeding an RD:ND (where ND is normal direction) aspect ratio of 30 [21]. For the sample annealed at 500 °C, the layer size and interface morphology changed compared to the as-rolled sample, albeit slightly. The interfaces remain planar, apart from some spheriodizing in the finest Nb layers (see arrows) and formation of large crystallographic facets (also indicated by arrows). At 600 °C, the grains in many regions of the material have changed in shape, from elongated to spherical, as the grain boundaries migrate. At 700 °C, the fraction of the spherical grains increases. The thicknesses of most of the layers have also enlarged. Most of the interface regions in this case bear a wavy morphology. From 800 °C to 1000 °C, nearly all the grains inside the layers have become nearly spherical, and as a consequence, the Cu/Nb interface morphology over most of the material is undeniably wavy.

The TEM analysis identifies that the main process responsible for increases in layer thickness is spheroidization of the interlayer grains. Mobilization of the grain boundaries enables the grain shape change [22]. The Cu/Nb interfaces, in contrast, do not migrate as they are relative more thermally stable than the grain boundaries [22]. The Cu/Nb interfaces, instead, become curved to accommodate the grain spherodization and their atomic structure becomes comprised of a new set of atomic-scale facets to accommodate the curvature. As an example, Fig. 2h shows an example of a curve region of the Cu/Nb consisting of facets indexed as $(11\bar{1})Cu||(01\bar{1})Nb$ seen in the 800 °C exposed sample. This structure is different than the structure of the nominally planar Cu/Nb interface, which are also faceted, but with alternating {111}Cu//{110}Nb and {100}Cu//{110}Nb facets [23]. In the new curve morphology assumed under high temperatures, the interfaces achieve a locally lower energy states by faceting [5].

Table 1
Structure and property change via annealing temperature.

	As rolled	500 °C	600 °C	700 °C	800 °C	900 °C	1000 °C
Layer thickness (nm)	32 ± 21	43 ± 23	62 ± 28	101 ± 45	195 ± 82	281 ± 102	357 ± 162
Ultimate tensile strength (MPa)	1238	1137	1117	880	687	543	468
Elongation (%)	2.8	2.1	1.6	1.5	2.6	3.5	6.4

Based on the TEM results, two distinct annealing temperature regimes can be identified. The first corresponds to 500–700 °C, wherein the ultimate strength of the material does not change appreciably but ductility decreased with increasing temperature. The layer thickness has increased from 32 nm to 101 nm, but nonetheless remains nanoscale. The stored dislocation density in the layers likely has decreased, but the change is not noticeable (Fig. 3). The most prominent change over this annealing temperature range is roughening in the layer morphology from being flat at 500 °C to partially flat and wavy at 600 °C and mostly wavy at 700 °C. A reduction in ductility with a

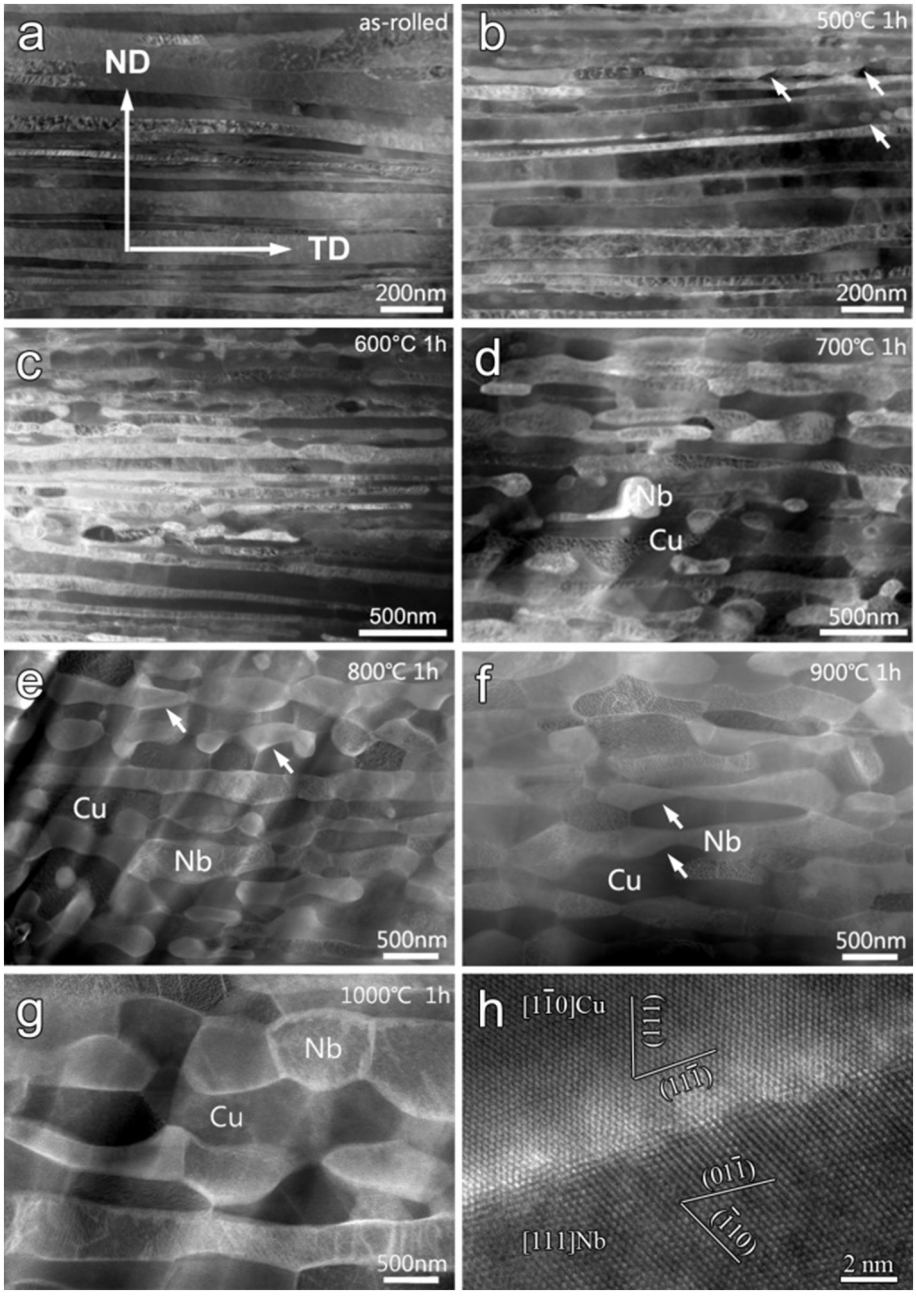

Fig. 2. Morphology change via annealing temperature. (a) the as-rolled sample shows plannar interfaces; (b-c) after annealing at 500 °C and 600 °C, the samples still display plannar interface but with locally faceting; (d-g) after annealing at 700 °C and above, the samples show notable roughness; (h) high resolution image of a typical facet shown in the 800 °C annealed sample (e).

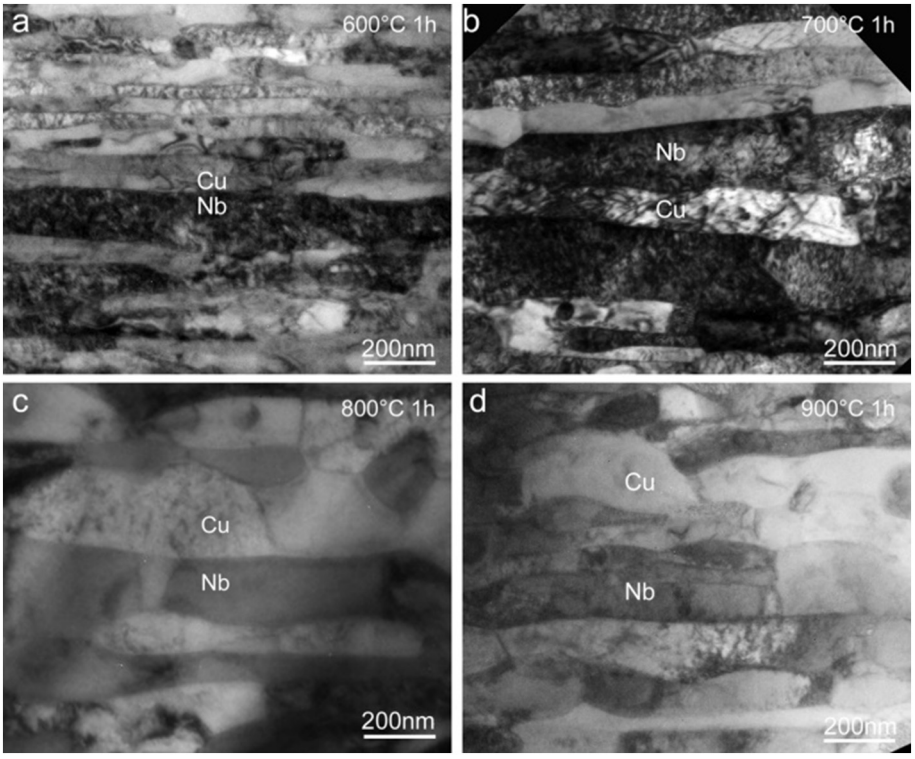

Fig. 3. Bright field TEM images showing a transition temperature 700 °C and 800 °C for dramatic dislocation density drop.

reduction in grain aspect ratio has been reported in nanocrystalline single phase materials [24,25]. However, in the nanolaminate case, the change in grain shape from highly planar to nearly spherical translates into an increase in layer roughness. The Cu/Nb interfaces become wavy at the mesoscale, with wavelengths on the order of submicrons. Higher interface roughness has been associated with reduced ductility, or elongation to failure in copper/bronze ARB processed laminates [26]. Albeit on a finer, nanoscale microstructure, we are likely observing a similar phenomenon in these temperature-roughened nanolaminates.

The second regime is associated with 800–1000 °C, wherein a dramatic drop in ultimate stress from those of the 700 °C annealed sample was observed, as well as increasing elongation to failure with increasing annealing temperature. The drop can be explained by the outstandingly large changes in layer thickness H, dislocation density, and grain shape occurring between 700 °C to 800 °C. A noticeable two-fold increase in H occurs from 700 °C to 800 °C. As shown in Fig. 3, from 700 to 800 °C, we find the greatest increase in the fraction of interlayer grains that change from grains with high aspect ratios of ~10, to small aspect ratios of nearly 1–2. Also, from Fig. 3, we see that another remarkable change occurring particularly between the 700 to 800 °C annealing temperatures is a dramatic drop in dislocation density. The increase in layer thickness and grain size as well decrease in intergranular dislocation density increase the obstacle spacing for gliding dislocations leading to reduced strength.

The increase in layer thickness H due to annealing will affect Cu/Nb strength. In nanolaminates, the main characteristic length scale determining strength is the layer thickness, or the spacing between biphase interfaces [14]. Interfaces serve as barriers that restrict the nucleation and constrain propagation of gliding dislocations [14]. For as-rolled material, it has been shown that the layer size scaling of strength follows a Hall-Petch law with a scaling factor corresponding to that for Cu [19]. In the present case, average layer thickness is altered due to annealing and not deformation. While a single crystal still spans the layer between two adjacent interfaces, the annealing-affected interfaces have been roughened, while as-rolled interfaces are planar. In Fig. 4, we plot the layer size scaling of strength on a Hall-Petch plot for two groups of ARB Cu/Nb nanolaminates. One group has been annealed at temperatures from 600 to 1000 °C with morphologically wavy interfaces and the other group consist of the ARB Cu/Nb annealed at 500 °C and as rolled ARB Cu/Nb nanolaminates with planar, or flat interfaces [19]. First, it is noteworthy that the strength of the wavy interface group also follows well the Hall-Petch scaling law, $\sigma = \sigma_0 + KH^{-1/2}$, where σ is the tensile strength and K is the coefficient. Quantitatively the Hall-Petch relations are found to follow $\sigma_{wavy} = 37.71 + 8536 \times H^{-1/2}$ and $\sigma_{flat} = 606.59 + 3313 \times H^{-1/2}$, subscripts wavy and flat indicate the two groups of samples. Clearly, the ARB Cu/Nb nanolaminates

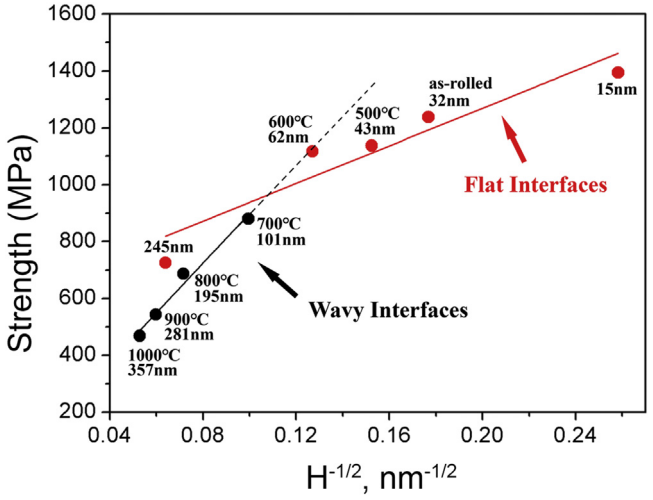

Fig. 4. H–P relations of ARB Cu/Nb nanolaminates with wavy and flat interfaces, respectively. The strength of ARB Cu/Nb nanolaminates with layer thickness of 15 and 245 nm is cited from ref. [19].

with wavy interfaces exhibits a much stronger size scaling than that of the ARB Cu/Nb nanolaminates with flat interfaces.

The different K for the two group materials can be attributed to their structure features. After exposed to extremely high temperature, the layers remain continuous and the layer thickness H remains nanoscale. So generally the tensile strength of ARB Cu/Nb nanolaminates still follows the strength scaling law in H. This agrees with a recent viewpoint that Hall-Petch with modified coefficients provides a good fit down to layer thicknesses of about 5 nm, although this length scale overlaps with that predict by CLS theory [13]. However, other microstructural features, particularly the interface morphology, also change. The wavy interfaces, with undulating surfaces could pose an even greater barrier to slip transmission. Thus, the group with wavy interfaces shows a higher coefficient of the Hall-Petch law.

In summary, microstructural evolution and strength and ductility induced by extreme temperature annealing in nanolayered ARB Cu/Nb composites has been investigated. With a critical annealing temperature of 700 °C, the Cu/Nb interface transforms from flat to wavy, the layer thickness increases but remains continuous, the intralayer grain size aspect ratio decreases, and the dislocation density reduces. Remarkably of all the changes observed to take place, the tensile strength is linearly proportional to $H^{-1/2}$. However, the slope of the H—P law, that indicates the sensitive of strength to H, is affected significantly by interface morphology. The wavy interfaces induced from extreme temperature exposure gives rise to a stronger size scaling. We rationalize this result can be attributed to greater resistance to slip transmission across wavy interfaces compared to planar, flat interfaces. Last, the sample annealed at 1000 °C, nearly the melting temperature of Cu, for 1 h still has a high strength (468 MPa), and high elongation of 6.4%.

Acknowledgements

This work was supported financially by the “Hundred Talents Project” of Chinese Academy of Sciences, the “Thousand Youth Talents Plan” of China, the National Natural Science Foundation of China (No. 51771201), and the Shenyang National Laboratory for Materials Science (No. 2017RP17). I.J.B acknowledges support by the U.S. Dept. of Energy, Office of Basic Energy Sciences Program DE-SC0018901.

References

[1] S. Zheng, I.J. Beyerlein, J.S. Carpenter, K. Kang, J. Wang, W. Han, N.A. Mara, Nat. Commun. 4 (2013) 1696.
[2] I.J. Beyerlein, N.A. Mara, J.S. Carpenter, T. Nizolek, W.M. Mook, T.A. Wynn, R.J. McCabe, J.R. Mayeur, K. Kang, S.J. Zheng, J. Wang, T.M. Pollock, J. Mater. Res. 28 (2013) 1799–1812.
[3] J.S. Carpenter, S.J. Zheng, R.F. Zhang, S.C. Vogel, I.J. Beyerlein, N.A. Mara, Philos. Mag. 93 (2013) 718–735.
[4] S.J. Zheng, J.S. Carpenter, R.J. McCabe, I.J. Beyehein, N.A. Mara, Sci. Rep. 4 (2014) 4226.
[5] S. Zheng, J.S. Carpenter, J. Wang, N.A. Mara, I.J. Beyerlein, Appl. Phys. Lett. 105 (2014) 111901.
[6] A. Misra, R.G. Hoagland, H. Kung, Philos. Mag. 84 (2004) 1021–1028.
[7] F. Moszner, C. Cancellieri, M. Chiodi, S. Yoon, D. Ariosa, J. Janczak-Rusch, L.P.H. Jeurgens, Acta Mater. 107 (2016) 345–353.
[8] J.B. Dubois, L. Thilly, P.O. Renault, F. Lecouturier, M. Di Michiel, Acta Mater. 58 (2010) 6504–6512.
[9] L.P. Deng, K. Han, B.S. Wang, X.F. Yang, Q. Liu, Acta Mater. 101 (2015) 181–188.
[10] G. Badinier, C.W. Sinclair, S. Allain, O. Bouaziz, Mater. Sci. Eng. A 597 (2014) 10–19.
[11] L.P. Deng, B.S. Wang, H.L. Xiang, X.F. Yang, R.M. Niu, K. Han, Acta Metall. Sin.-Engl. 29 (2016) 668–673.
[12] L.P. Deng, B.S. Wang, K. Han, R.M. Niu, H.L. Xiang, K.T. Hartwig, X.F. Yang, J. Mater. Sci. 54 (2019) 840–850.
[13] S. Subedi, I.J. Beyerlein, R. Lesar, A.D. Rollett, Scr. Mater. 145 (2018) 132–136.
[14] A. Misra, J.P. Hirth, R.G. Hoagland, Acta Mater. 53 (2005) 4817–4824.
[15] N. Hansen, Scr. Mater. 51 (2004) 801–806.
[16] S.J. Zheng, J. Wang, J.S. Carpenter, W.M. Mook, P.O. Dickerson, N.A. Mara, I.J. Beyerlein, Acta Mater. 79 (2014) 282–291.
[17] N. Li, J. Wang, A. Misra, J.Y. Huang, Microsc. Microanal. 18 (2012) 1155–1162.
[18] J. Wang, C.Z. Zhou, I.J. Beyerlein, S. Shao, JOM 66 (2014) 102–113.
[19] T. Nizolek, I.J. Beyerlein, N.A. Mara, J.T. Avallone, T.M. Pollock, Appl. Phys. Lett. 108 (2016), 051903.
[20] S.C. Jha, R.G. Delagi, J.A. Forster, P.D. Krotz, Metall. Trans. A. 24 (1993) 15–20.
[21] I.J. Beyerlein, J.R. Mayeur, R.J. McCabe, S.J. Zheng, J.S. Carpenter, N.A. Mara, Acta Mater. 72 (2014) 137–147.
[22] A. Misra, R.G. Hoagland, J. Mater. Res. 20 (2005) 2046–2054.
[23] S.J. Zheng, I.J. Beyerlein, J. Wang, J.S. Carpenter, W.Z. Han, N.A. Mara, Acta Mater. 60 (2012) 5858–5866.
[24] Y.M. Wang, E. Ma, Acta Mater. 52 (2004) 1699–1709.
[25] G.J. Fan, H. Choo, P.K. Liaw, Appl. Phys. Lett. 89 (2006) 1012.
[26] X. Ma, C. Huang, J. Moering, M. Ruppert, H.W. Höppel, M. Göken, J. Narayan, Y. Zhu, Acta Mater. 116 (2016) 43–52.